JACS
JOURNAL OF THE AMERICAN CHEMICAL SOCIETY
pubs.acs.org/JACS
Article

Chemical Tuning of Fibers Drawn from Extensible Hyaluronic Acid Networks

Crystal K. Chu, Alby J. Joseph, Matthew D. Limjoco, Jiawei Yang, Suman Bose, Lavanya S. Thapa, Robert Langer, and Daniel G. Anderson*

Cite This: https://dx.doi.org/10.1021/jacs.0c09691
Read Online

ABSTRACT: Polymer fibers with specific chemical and mechanical properties are key components of many biomaterials used for regenerative medicine and drug delivery. Here, we develop a bioinspired, low-energy process to produce mechanically tunable biopolymer fibers drawn from aqueous solutions. Hyaluronic acid (HA) forms dynamic cross-links with branched polyethylene glycol polymers end-functionalized with boronic acids of varied structure to produce extensible polymer networks. This dynamic fiber precursor (DFP) is directly drawn by pultrusion into HA fibers that display high aspect ratios, ranging from 4 to 20 μm in diameter and up to ∼10 m in length. Dynamic rheology measurements of the DFP and tensile testing of the resulting fibers reveal design considerations to tune the propensity for fiber formation and fiber mechanical properties, including the effect of polymer structure and concentration on elastic modulus, tensile strength, and ultimate strain. The materials' humidity-responsive contractile behavior, a unique property of spider silks rarely observed in synthetic materials, highlights possibilities for further biomimetic and stimulus-responsive fiber applications. This work demonstrates that chemical modification of dynamic interactions can be used to tune the mechanical properties of pultrusion-based fibers and their precursors.

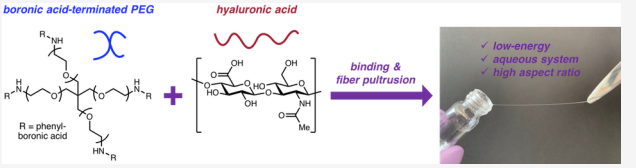

INTRODUCTION

Naturally sourced and synthetic polymer fibers are important structural components in textiles, composite materials, and soft materials for biomedical applications.[1−3] Fibrous structures provide spatial orientation and porosity needed for cell migration and transport of air and nutrients, which are critical for biomaterials such as bandages, implants, and engineered tissues.[4,5] Natural fibers have inspired the development of biomimetic materials based on engineered and reprocessed silks that have been widely applied in regenerative medicine and drug delivery systems.[6,7] Showcased by spider and silkworm silks, macroscopic fibers are produced by Nature with efficiencies and mechanical properties that remain unmatched by artificial silk spinning methods.[8] Furthermore, traditional methods for synthetic fiber production also face challenges in processing and biocompatibility. Polymer fiber synthesis, particularly for hydrophilic polymers, is often burdened by high energy costs and limited by the operational difficulty of extruding viscous polymer solutions.[9,10] In well-established methods such as electrospinning, the reliance on and removal of potentially toxic organic solvents remain as challenges.[11] Polymers such as polycaprolactone that sacrifice wettability for mechanical strength are predominantly used, and redesigning or coating of hydrophobic fibers must be performed prior to medical application.[12]

Studies of spider and silkworm silk production suggest that the pulling force exerted by movement or weight of the animal may be more crucial for fiber formation than the shear forces observed in the spinning duct.[8] Similar to natural silk spinning, the fiber formation in this study relies on mechanical pultrusion from a water-based fluid precursor free of high voltage, elevated temperature, or organic solvents. Previous reports of fiber production from aqueous networks and composites have been shown to occur via self-assembly, resulting in fibers typically on length scales ranging from submicrometers to centimeters.[13,14] Rare examples of nanoparticle/polymer networks based on physical interactions or irreversible covalent bonds have been reported to form fibers by pultrusion.[9,15,16] However, fiber pultrusion from aqueous networks of biopolymers remains limited.[9] Furthermore, developing systems that can be chemically tuned to afford ranges of mechanical properties characteristic of distinct biological materials requires further investigation.

Here, we describe an operationally simple, low-energy method to prepare polymer fibers from aqueous solutions. Hyaluronic acid (HA) and boronic acid-terminated branched polymers form networks through dynamic cross-links, resulting

Received: September 9, 2020

https://dx.doi.org/10.1021/jacs.0c09691
J. Am. Chem. Soc. XXXX, XXX, XXX−XXX

in fluid, dynamic fiber precursors (DFPs) that can be drawn into dry, macroscopic fibers meters in length. HA was the primary focus of this study due to its prevalence in synthetic biomaterials and in biological systems, such as the extracellular matrix, and to address challenges in electrospinning protocols caused by hydrophilicity and high viscosity.[10,17,18] By modifying the chemical substituents and concentration of the boronic acid-functionalized polymer, structural changes to the polymers were correlated with effects on the rheological properties of the DFPs and mechanical properties of the HA fibers. These structure−property relationships are expected to facilitate the expansion of this method as a general approach for the production of bioinspired, mechanically tunable polymer fibers under low-energy and aqueous conditions. Fiber pultrusion from DFPs represents an unexplored strategy toward the manufacturing of biomimetic materials, including artificial muscles and chemoresponsive sensors.

RESULTS AND DISCUSSION

Preparation of DFP Library and Polymer Fibers. Polymer fibers were fabricated by first preparing bulk DFPs composed of two polymeric components. Low molecular weight (5 kDa), 4-arm branched polyethylene glycol polymers (PEGs) were end-functionalized with phenylboronic acids (PBAs) and served as dynamic cross-linkers of high molecular weight HA (Figure 1).[19] Previous studies have suggested that

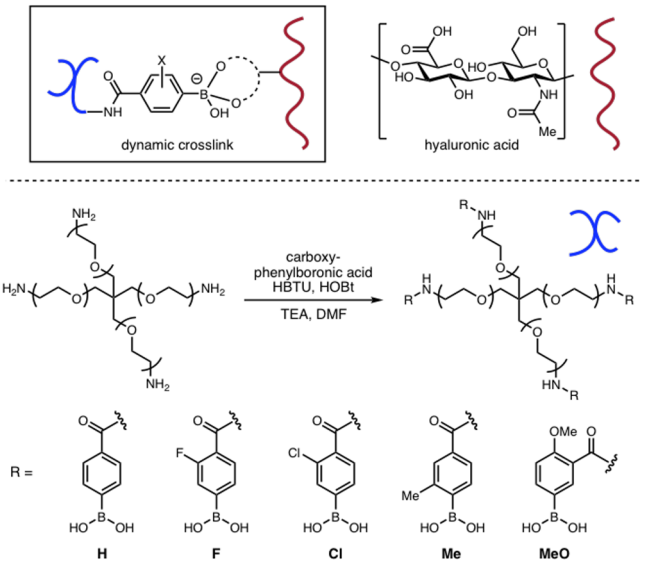

Figure 1. Proposed binding interaction between HA and branched PEG−PBA favored under basic conditions, and synthetic route for PEG−PBAs containing various chemical substituents on the phenyl ring (H, F, Cl, Me, MeO).

boronic acid complexation has the potential to form dynamic networks of HA and other polysaccharides, which are common building blocks of biomaterials due to their natural abundance and biocompatibility.[20−22] A library of five PEG−PBAs was prepared by varying chemical substitution on the phenyl rings of the PBA to investigate the effect of chemical structure on material properties; both electron-withdrawing and -donating groups were introduced, including fluoro (F), chloro (Cl), methyl (Me), and methoxy (MeO) substituents, in addition to the unsubstituted analog (H). Mixing each PEG−PBA separately with HA in solution under basic conditions led to formation of a viscous, extensible fluid, the DFP, that could be easily drawn into dry cylindrical fibers ranging from 4 to 20 μm in diameter (Figure 2a and 2b).

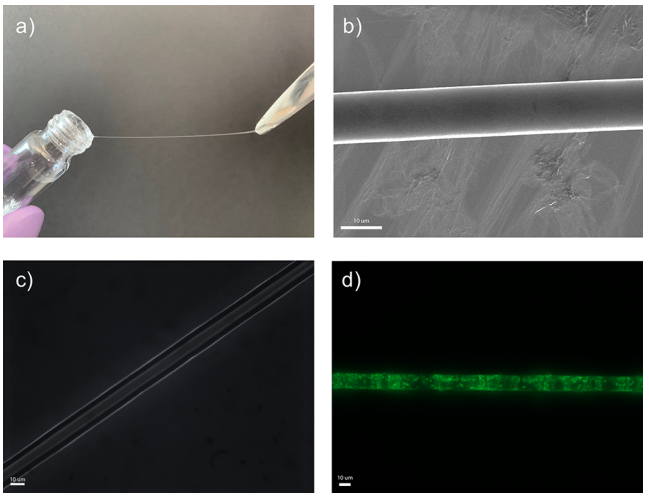

Figure 2. (a) Photograph of a fiber drawn from a DFP. (b) SEM image of a dry fiber. (c) Polarized light microscopy of a birefringent fiber oriented at ∼45° between crossed polarizers. (d) Microscope image of a fiber drawn from a DFP containing 2 μm fluorescent particles. Scale bars represent 10 μm.

Attempts to form DFPs without the presence of PBA functional groups suggest that fiber formation is dependent on dynamic interactions between the PEG−PBA and HA, which likely result in covalent cross-links. When the branched PEG was left unfunctionalized as PEG−OH, unmodified as the commercially available starting material PEG−NH_2, or terminated with a different functional group such as maleimide (PEG−MAL), fibers could not be drawn from the fluids derived from mixing with HA, consistent with boronic acid complexation being a requirement for fiber formation. Furthermore, with the ratio of PBA to HA disaccharide repeat units held constant, changes to the extent of branching in the PEG polymer did not prohibit fiber formation, and fibers could be drawn using both 8-arm and linear PEG−PBAs. Solutions of alginate could be used in place of HA to prepare chemically distinct DFPs that also yield polymer fibers.[21] Production of fibers containing HA and alginate demonstrates how this process could serve as a general method for the fabrication of fibers drawn from dynamic networks of polysaccharides.

The pulling force exerted on the bulk fluid needed for fiber formation could be achieved manually or with a motorized pump and likely causes polymer alignment during fiber formation (Video S1, Supporting Information). Polarized light microscopy was used to provide insight into the structural changes resulting from these processing conditions (Figure 2c). When a fiber was oriented ∼45° relative to the polarizer and analyzer, peak birefringence was observed, whereas at 0°and 90°, birefringence was minimized, suggesting an anisotropic orientation of polymer chains along the fiber axis.[14,23] Inspired by cargo-loaded hydrogels for drug delivery, we next attempted to prepare fibers from DFPs formulated with microparticles to determine if extensibility and the pultrusion process would be affected.[24,25] Fluorescent microparticles mixed into the DFP did not disrupt fiber drawing, allowing for generation of fibers containing particles dispersed

https://dx.doi.org/10.1021/jacs.0c09691
J. Am. Chem. Soc. XXXX, XXX, XXX−XXX

throughout the material (Figure 2d). The ease of preparing particle-loaded fibers demonstrates the utility of this method for the manufacturing of composite materials tailored to mechanical and drug delivery applications.

Dynamic Rheology of DFP Library and Effects on Draw Length. Rheological studies were performed to evaluate how the chemical modifications in the PEG library influence the properties of the various DFPs and affect fiber formation (Figure 3). We hypothesized that the electronic effects of

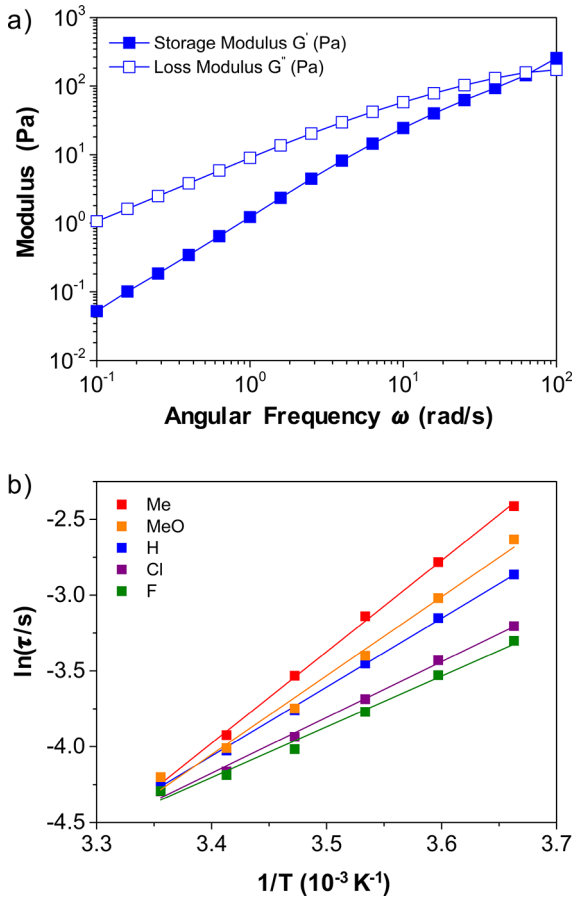

Figure 3. (a) Representative dynamic oscillatory frequency sweep measurement of the DFP containing unsubstituted PEG−PBA (H) at 25 °C. (b) Overlay of Arrhenius plots for DFPs prepared from a library of PEG−PBAs in order of decreasing $E_{a,dissociation}$.

substituents on the PBA would affect the mechanical properties of the DFP, thereby influencing the propensity for fiber formation. Previous studies of PBA-based cross-linking suggest that PBAs with lower pK_a promote cross-link formation, citing the mechanism of boronic acid−diol complexation which is enabled by formation of the boronate anion.[19,26] Each PEG−PBA was mixed with HA to form five chemically distinct DFPs, and strain-dependent oscillatory rheology was performed for each fluid to locate the linear viscoelastic regions (Figure S1, Supporting Information). Dynamic oscillatory frequency sweep measurements were then performed within the linear viscoelastic region and the crossover frequencies compared for each DFP (Figure 3a). The crossover frequency, at which the storage modulus G' and loss modulus G'' curves intersect, represents the barrier between liquid-like ($G' < G''$) and solid-like ($G' > G''$) behavior and can be used as a measure of gel strength in dynamic networks.[19,27] The reciprocal of this crossover frequency provides the relaxation time τ, or the time scale for the material to flow due to cross-link dissociation. Despite the incorporation of different chemical substituents on the PBA, the range of observed crossover frequencies and relaxation times at 25 °C was narrow across all DFPs prepared from the PEG−PBA library.

While the relaxation times for the DFPs at 25 °C were not greatly altered by varying chemical substitution on the PBAs, the temperature dependence of the measured relaxation times was determined to investigate the kinetics of cross-link dissociation. For each DFP containing a different chemical modification in the PEG−PBA library, dynamic frequency sweep measurements were performed at five temperatures and the relaxation times calculated at each temperature. Plotting the temperature dependence of relaxation times for each DFP according to eq 1 revealed Arrhenius relationships (Figure 3b). In each case, the activation energy of cross-link dissociation ($E_{a,dissociation}$) was calculated from the slope of the line of best fit using the Arrhenius equation.[28,29] The Arrhenius plots indicate the significant influence of the electronic effects of the PBA chemical substituents on cross-link dissociation, consistent with dynamic interactions between the PBAs and HA; the electron-donating groups tested lead to higher $E_{a,dissociation}$, while the electron-withdrawing groups tend to decrease the activation energy.

$$\ln \tau = \frac{E_a}{kT} + \ln \tau_0 \quad (1)$$

As cross-link dissociation was expected to be an important factor in fiber drawing, we next determined the relationship between PBA chemical substitution and fiber draw length, a measure of the extensibility of the DFP (Figure 4a). The maximum linear draw length was estimated by drawing 10 fibers from each polymer mixture. The DFPs containing PBAs with methyl (Me) or methoxy (MeO) substituents, which have the highest values of $E_{a,dissociation}$, could be drawn to form fibers between 1 and 3 m long. In comparison, draw lengths for materials containing the unsubstituted PBA (H) or those with electron-withdrawing groups reached greater than 5 m in length. These data suggest that a low energy barrier to cross-link dissociation, which can allow for a highly dynamic and more extensible DFP, favors longer fiber draw lengths.

The molar ratio of the two polymeric components, PEG and HA, could also be altered to tune fiber properties. The unsubstituted PEG−PBA (H) was combined with HA in one-half ($0.5x$) and twice ($2x$) the loading as compared to the standard procedure ($1x$, where $x \approx 2$ PBA moieties per HA disaccharide repeat unit). As PEG−PBA loading decreases, the diameter of the resulting fiber also decreases. One possible explanation for this relationship is that the lower concentration of PBA moieties leads to fewer cross-links per HA polymer to form a thinner fiber. Furthermore, it was determined that PEG−PBA loading inversely correlates with maximum fiber draw length (Figure 4b). In the case where PEG−PBA loading was reduced to one-half of that of the standard procedure, fiber draw length reached over 10 m, 2−40 times longer than previously reported for organic solvent-free nanocomposite gels, indicating the potential scalability of this method toward efficient fabrication of fibrous biomaterials.[9,15]

Effects of Chemical Substituent and Polymer Ratio on Fiber Mechanical Properties. Deciphering the relationships between molecular structure and mechanical properties,

https://dx.doi.org/10.1021/jacs.0c09691
J. Am. Chem. Soc. XXXX, XXX, XXX−XXX

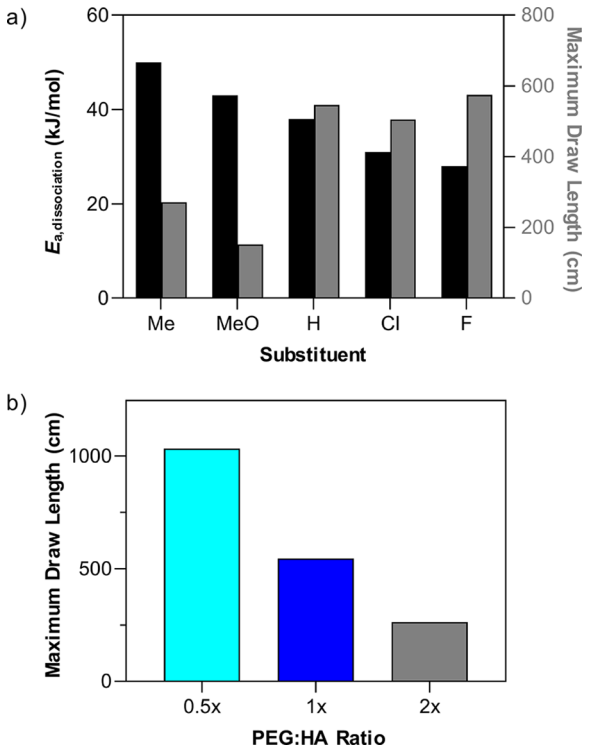

Figure 4. (a) Dependence of $E_{a,dissociation}$ and maximum fiber draw length (of 10 experiments) on the PBA chemical substituent. (b) Dependence of maximum fiber draw length (of 10 experiments) on the ratio of polymeric components, where x is defined as the molar ratio of PBA moieties (4 per PEG molecule) to HA disaccharide repeat units, ~2.

such as elastic modulus, ultimate strain, and tensile strength, is vital to producing biomaterials suited for particular biomedical applications.[30−32] Tensile testing of single fibers was conducted to investigate the mechanical differences caused by varying the PBA chemical substituents and the ratio of the polymeric components used to prepare the DFP. The stress−strain profiles for three fiber compositions with varied chemical substitution on the PBA (Me, H, F) are summarized in Figure 5 (see Figure S3 in the Supporting Information for an overlay of stress−strain profiles). In most cases, increasing the strain rate did not lead to brittle fracture. Tensile strength and ultimate strain averaged ~5−6 MPa and ~50−60% strain for fibers containing fluorinated and unsubstituted PEG−PBAs, while the fiber containing methylated PEG−PBA showed a higher tensile strength and much lower failure strain (Figure 5a−c). Changing the chemical substitution of a single site on the PBA also provides access to polymer fibers with a wide range of values for elastic modulus. Use of the methylated PBA, which formed the DFP with the highest activation energy of cross-link dissociation, provided fibers with high elastic modulus (~119 MPa), whereas substitution with the electron-withdrawing fluoride group resulted in fibers with lower modulus (~6 MPa) (Figure 5d). Furthermore, repeated loading−unloading cycles at low strain of a fiber containing methylated PBA revealed a high initial dissipation energy as well as high residual strain and weakening of the mechanical properties in subsequent cycles (Figure S4, Supporting Information). In contrast, a fiber containing fluorinated PBA exhibited a lower dissipation energy and relatively stable mechanical properties. Modification of the chemical substituent on a single site of the PBA provides a simple strategy to tune fiber mechanical properties for diverse applications.

The molar ratio of the PEG and HA components can be easily altered without synthetic effort to effectively change the cross-link density. We investigated the effect of the polymer ratio on fiber stress−strain profiles with the goal of developing a facile route to tune the fiber mechanical properties (Figure 5e, see Figure S5 in the Supporting Information for an overlay of the stress−strain profiles). Fibers were drawn from DFPs containing the unsubstituted PEG−PBA (H) mixed with HA in the standard ratio ($1x$), at one-half the PEG−PBA loading ($0.5x$), and using double the standard amount of cross-linker ($2x$). The highest values of tensile strength and elastic modulus were measured for fibers with the lowest polymer ratio, with significantly increased values observed when PEG loading was decreased from the standard ratio to $0.5x$ (Figure 5f and 5h). These trends could be explained by the increased ratio of cross-linked versus free PEG arms and the greater number of available HA sites to accommodate PBA cross-linking, favoring formation of an extended polymer network. As the PEG polymers have four branches and PBA functionalities, the loading of PEG−PBA used in the standard procedure includes ~2 PBA functional groups for each HA disaccharide repeat unit. As PEG loading is increased, high concentrations of PEG can crowd the HA binding sites and inhibit network formation, one possible reason for decreased mechanical strength. When comparing the mechanical properties at strain rates of 10 and 50 mm/min, the fiber with the lowest ratio ($0.5x$) was the only case tested in which tensile strengths were significantly greater at higher strain rate, reaching tensile strengths up to 50 MPa (Figure S6, Supporting Information). Modification of the ratio of the two polymeric components provides an operationally simple method for tuning fibers across a wide range of mechanical properties without the need for further synthetic manipulation of the constituent polymers.

Humidity-Responsive Contractile Behavior. The dynamic cross-links that enable fiber formation by pultrusion give rise to unique stimulus-responsive properties, as demonstrated by the humidity-responsive behavior of the fibers (Figure 6). Upon exposure to humidity, a suspended polymer fiber contracts, shrinking to ~25% of its original length in 15 min.

Supercontraction in response to humidity is a known property of spider silks rarely observed in other materials.[33] Following polymer alignment and drying during the fiber drawing process, reintroduction of water can disrupt the fiber structure, allowing for entropically favorable reorientation of the polymers and fiber contraction.[34] The fibers' contractile behavior was utilized for weightlifting applications (Video S2, Supporting Information). A bundle of five fibers lifted an 8 mg load approximately 10 mm over the course of 4 min in a humid chamber (Figure S9, Supporting Information). Given their hydrophilicity and absence of secondary cross-linking, the fibers reported herein are predictably susceptible to dissolution under aqueous conditions, serving as a potential strategy for material recycling and degradation. In addition to its biocompatibility, HA is easily functionalized, suggesting that our production method is well suited for secondary cross-linking approaches to facilitate biomedical applications. Studies to enhance the persistence of the HA fibers in physiological conditions are underway.

https://dx.doi.org/10.1021/jacs.0c09691
J. Am. Chem. Soc. XXXX, XXX, XXX−XXX

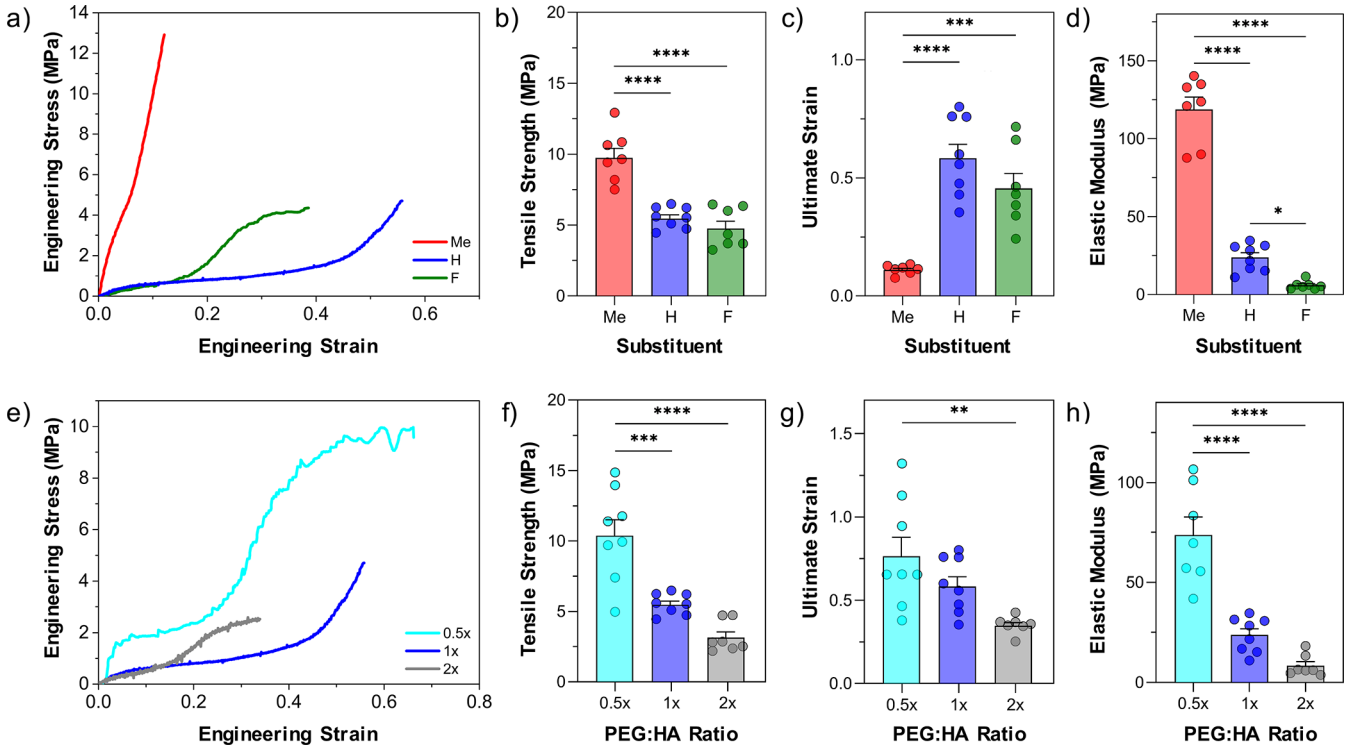

Figure 5. (a) Representative stress−strain profiles measured using a 10 mm/min strain rate for fibers with varied chemical substitution on the PEG−PBA. (b−d) Data sets for tensile strength, ultimate strain, and elastic modulus for samples of three fiber types, each containing a different PBA chemical substituent: methyl (Me), unsubstituted (H), and fluoro (F). (e) Representative stress−strain profiles measured using a 10 mm/min strain rate for fibers with varied polymer ratios. (f−h) Data sets for tensile strength, ultimate strain, and elastic modulus for samples of three fiber types, each containing a different ratio of PEG:HA. x is defined as in Figure 4. Bar heights and error bars represent means + SEM, while dots represent measured values for individual fibers; n = 7 or 8 for each fiber type. One-way ANOVA and post-hoc Tukey test were performed to determine statistical significance. Statistically significant differences in data sets are labeled: $^{*}P \leq 0.05$, $^{**}P \leq 0.01$, $^{***}P \leq 0.001$, and $^{****}P \leq 0.0001$. $P > 0.05$ is considered not significant.

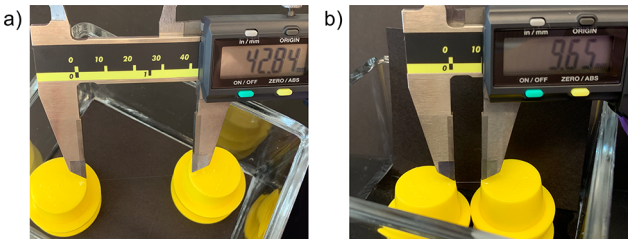

Figure 6. Polymer fiber (a) before and (b) after supercontraction resulting from increased humidity. Initial length is ∼43 mm; length after 15 min is ∼10 mm.

CONCLUSIONS

We developed a low-energy, organic solvent-free method to produce fibers from extensible fluids based on HA and boronic acid-terminated PEGs. Fibers containing alginate in place of HA were also formed, suggesting that this strategy could potentially be used to access a variety of polysaccharide fibers. Following preparation of a library of DFPs involving systematic variation of the PBA chemical structure and the molar ratio of polymeric components, dynamic rheology and tensile testing experiments revealed structure−property relationships and design principles for fibers with tunable mechanical properties, including tensile strength, ultimate strain, and elastic modulus. This method produces fibers by pultrusion with high aspect ratios and longer length scales than previously reported for related physically cross-linked aqueous systems by reaching draw lengths 2−40 times greater, a feature that could facilitate application to large-scale production. The dynamic polymer networks present in the fibers provide opportunities for unique biomimetic properties, shown by the humidity-responsive, contracting, and weightlifting properties of the HA fibers. This study demonstrates a strategy for chemically tuning the mechanical properties of biopolymer fibers that represent a promising class of materials for transformative medical technologies.

ASSOCIATED CONTENT

Supporting Information

The Supporting Information is available free of charge at https://pubs.acs.org/doi/10.1021/jacs.0c09691.

Procedures and characterization data (PDF)

Pultrusion process (mp4)

Weightlifting demonstration (mp4)

AUTHOR INFORMATION

Corresponding Author

Daniel G. Anderson − *David H. Koch Institute for Integrative Cancer Research, Department of Chemical Engineering, and Harvard-Massachusetts Institute of Technology Division of Health Sciences and Technology, Institute for Medical Engineering and Science, Massachusetts Institute of Technology, Cambridge, Massachusetts 02139, United States;* orcid.org/0000-0003-0151-4903; Email: dgander@mit.edu

https://dx.doi.org/10.1021/jacs.0c09691
J. Am. Chem. Soc. XXXX, XXX, XXX−XXX

Authors

Crystal K. Chu − *David H. Koch Institute for Integrative Cancer Research, Massachusetts Institute of Technology, Cambridge, Massachusetts 02139, United States;* orcid.org/0000-0002-7783-2564

Alby J. Joseph − *David H. Koch Institute for Integrative Cancer Research, Massachusetts Institute of Technology, Cambridge, Massachusetts 02139, United States*

Matthew D. Limjoco − *David H. Koch Institute for Integrative Cancer Research, Massachusetts Institute of Technology, Cambridge, Massachusetts 02139, United States; Department of Anesthesiology, Critical Care and Pain Medicine, Boston Children's Hospital, Boston, Massachusetts 02115, United States*

Jiawei Yang − *David H. Koch Institute for Integrative Cancer Research, Massachusetts Institute of Technology, Cambridge, Massachusetts 02139, United States; Department of Anesthesiology, Critical Care and Pain Medicine, Boston Children's Hospital, Boston, Massachusetts 02115, United States*

Suman Bose − *David H. Koch Institute for Integrative Cancer Research, Massachusetts Institute of Technology, Cambridge, Massachusetts 02139, United States*

Lavanya S. Thapa − *David H. Koch Institute for Integrative Cancer Research, Massachusetts Institute of Technology, Cambridge, Massachusetts 02139, United States; Department of Anesthesiology, Critical Care and Pain Medicine, Boston Children's Hospital, Boston, Massachusetts 02115, United States*

Robert Langer − *David H. Koch Institute for Integrative Cancer Research, Department of Chemical Engineering, and Harvard-Massachusetts Institute of Technology Division of Health Sciences and Technology, Institute for Medical Engineering and Science, Massachusetts Institute of Technology, Cambridge, Massachusetts 02139, United States;* orcid.org/0000-0003-4255-0492

Complete contact information is available at: https://pubs.acs.org/10.1021/jacs.0c09691

Notes

The authors declare no competing financial interest.

■ ACKNOWLEDGMENTS

We thank Dr. Steven Kooi, Dr. Niels Holten-Andersen, Florence Müller, Dr. Katy Newlin, and Dr. Meri Treska for helpful discussions. This work was supported by a grant from the Leona M. and Harry B. Helmsley Charitable Trust (2017PG-T1D027). C.K.C. is grateful for support from the NIH through a postdoctoral fellowship (F32DK118785). S.B. is grateful for support from the NIH (K99EB025254) and a JDRF Postdoctoral Fellowship (PDF-2015-90-A-N). This work was supported in part by the Koch Institute Support (core) Grant P30-CA14051 from the National Cancer Institute. We thank the Koch Institute Swanson Biotechnology Center for technical support, specifically the Nanotechnology Materials Core Facility.

■ REFERENCES

(1) Smitthipong, W.; Suethao, S.; Shah, D.; Vollrath, F. Interesting Green Elastomeric Composites: Silk Textile Reinforced Natural Rubber. *Polym. Test.* **2016**, *55*, 17−24.

(2) Murugan, R.; Ramakrishna, S. Nano-Featured Scaffolds for Tissue Engineering: A Review of Spinning Methodologies. *Tissue Eng.* **2006**, *12*, 435−447.

(3) Davidson, M. D.; Ban, E.; Schoonen, A C. M.; Lee, M.-H.; D'Este, M.; Shenoy, V. B.; Burdick, J. A. Mechanochemical Adhesion and Plasticity in Multifiber Hydrogel Networks. *Adv. Mater.* **2020**, *32*, 1905719.

(4) Barnes, C. P.; Sell, S. A.; Boland, E. D.; Simpson, D. G.; Bowlin, G. L. Nanofiber Technology: Designing the Next Generation of Tissue Engineering Scaffolds. *Adv. Drug Delivery Rev.* **2007**, *59*, 1413−1433.

(5) Weng, L.; Xie, J. Smart Electrospun Nanofibers for Controlled Drug Release: Recent Advances and New Perspectives. *Curr. Pharm. Des.* **2015**, *21*, 1944−1959.

(6) Omenetto, F. G.; Kaplan, D. L. New Opportunities for an Ancient Material. *Science* **2010**, *329*, 528−531.

(7) Aigner, T. B.; DeSimone, E.; Scheibel, T. Biomedical Applications of Recombinant Silk-Based Materials. *Adv. Mater.* **2018**, *30*, 1704636.

(8) Mu, X.; Fitzpatrick, V.; Kaplan, D. L. From Silk Spinning to 3D Printing: Polymer Manufacturing Using Directed Hierarchical Molecular Assembly. *Adv. Healthcare Mater.* **2020**, *9*, 1901552.

(9) Wu, Y.; Shah, D. U.; Liu, C.; Yu, Z.; Liu, J.; Ren, X.; Rowland, M. J.; Abell, C.; Ramage, M. H.; Scherman, O. A. Bioinspired Supramolecular Fibers Drawn from a Multiphase Self-Assembled Hydrogel. *Proc. Natl. Acad. Sci. U. S. A.* **2017**, *114*, 8163−8168.

(10) Um, I. C.; Fang, D.; Hsiao, B. S.; Okamoto, A.; Chu, B. Electro-Spinning and Electro-Blowing of Hyaluronic Acid. *Biomacromolecules* **2004**, *5*, 1428−1436.

(11) Khorshidi, S.; Solouk, A.; Mirzadeh, H.; Mazinani, S.; Lagaron, J. M.; Sharifi, S.; Ramakrishna, S. A Review of Key Challenges of Electrospun Scaffolds for Tissue Engineering Applications. *J. Tissue Eng. Regener. Med.* **2016**, *10*, 715−738.

(12) Cipitria, A.; Skelton, A.; Dargaville, T. R.; Dalton, P. D.; Hutmacher, D. W. Design, Fabrication and Characterization of PCL Electrospun Scaffolds − A Review. *J. Mater. Chem.* **2011**, *21*, 9419−9453.

(13) Palmer, L. C.; Stupp, S. I. Molecular Self-Assembly into One-Dimensional Nanostructures. *Acc. Chem. Res.* **2008**, *41*, 1674−1684.

(14) Liu, Y.; Wang, T.; Huan, Y.; Li, Z.; He, G.; Liu, M. Self-Assembled Supramolecular Nanotube Yarn. *Adv. Mater.* **2013**, *25*, 5875−5879.

(15) Gaharwar, A. K.; Schexnailder, P. J.; Dundigalla, A.; White, J. D.; Matos-Pérez, C. R.; Cloud, J. L.; Seifert, S.; Wilker, J. J.; Schmidt, G. Highly Extensible Bio-Nanocomposite Fibers. *Macromol. Rapid Commun.* **2011**, *32*, 50−57.

(16) Dou, Y.; Wang, Z.-P.; He, W.; Jia, T.; Liu, Z.; Sun, P.; Wen, K.; Gao, E.; Zhou, X.; Hu, X.; Li, J.; Fang, S.; Qian, D.; Liu, Z. Artificial Spider Silk from Ion-Doped and Twisted Core-Sheath Hydrogel Fibres. *Nat. Commun.* **2019**, *10*, 5293.

(17) Ji, Y.; Ghosh, K.; Shu, X. Z.; Li, B.; Sokolov, J. C.; Prestwich, G. D.; Clark, R. A. F.; Rafailovich, M. H. Electrospun Three-Dimensional Hyaluronic Acid Nanofibrous Scaffolds. *Biomaterials* **2006**, *27*, 3782−3792.

(18) Wolf, K. J.; Kumar, S. Hyaluronic Acid: Incorporating the Bio into the Material. *ACS Biomater. Sci. Eng.* **2019**, *5*, 3753−3765.

(19) Yesilyurt, V.; Webber, M. J.; Appel, E. A.; Godwin, C.; Langer, R.; Anderson, D. G. Injectable Self-Healing Glucose-Responsive Hydrogels with pH-Regulated Mechanical Properties. *Adv. Mater.* **2016**, *28*, 86−91.

(20) Tarus, D.; Hachet, E.; Messager, L.; Catargi, B.; Ravaine, V.; Auzély-Velty, R. Readily Prepared Dynamic Hydrogels by Combining Phenyl Boronic Acid- and Maltose-Modified Anionic Polysaccharides at Neutral pH. *Macromol. Rapid Commun.* **2014**, *35*, 2089−2095.

(21) Hong, S. H.; Kim, S.; Park, J. P.; Shin, M.; Kim, K.; Ryu, J. H.; Lee, H. Dynamic Bonds between Boronic Acid and Alginate: Hydrogels with Stretchable, Self-Healing, Stimuli-Responsive, Re-moldable, and Adhesive Properties. *Biomacromolecules* **2018**, *19*, 2053−2061.

(22) Basu, A.; Kunduru, K. R.; Abtew, E.; Domb, A. J. Polysaccharide-Based Conjugates for Biomedical Applications. *Bioconjugate Chem.* **2015**, *26*, 1396−1412.
(23) Harrington, M. J.; Waite, J. H. pH-Dependent Locking of Giant Mesogen Fibers Drawn from Mussel Byssal Collagens. *Biomacromolecules* **2008**, *9*, 1480−1486.
(24) Gaharwar, A. K.; Peppas, N. A.; Khademhosseini, A. Nanocomposite Hydrogels for Biomedical Applications. *Biotechnol. Bioeng.* **2014**, *111*, 441−53.
(25) Chen, Q.; Wang, C.; Zhang, X.; Chen, G.; Hu, Q.; Li, H.; Wang, J.; Wen, D.; Zhang, Y.; Lu, Y.; Yang, G.; Jiang, C.; Wang, J.; Dotti, G.; Gu, Z. In Situ Sprayed Bioresponsive Immunotherapeutic Gel for Post-Surgical Cancer Treatment. *Nat. Nanotechnol.* **2019**, *14*, 89−97.
(26) Cambre, J. N.; Sumerlin, B. S. Biomedical Applications of Boronic Acid Polymers. *Polymer* **2011**, *52*, 4631−4643.
(27) Cromwell, O. R.; Chung, J.; Guan, Z. Malleable and Self-Healing Covalent Polymer Networks through Tunable Dynamic Boronic Ester Bonds. *J. Am. Chem. Soc.* **2015**, *137*, 6492−6495.
(28) Li, Q.; Barrett, D. G.; Messersmith, P. B.; Holten-Andersen, N. Controlling Hydrogel Mechanics *via* Bio-Inspired Polymer-Nanoparticle Bond Dynamics. *ACS Nano* **2016**, *10*, 1317−1324.
(29) Marco-Dufort, B.; Iten, R.; Tibbitt, M. W. Linking Molecular Behavior to Macroscopic Properties in Ideal Dynamic Covalent Networks. *J. Am. Chem. Soc.* **2020**, *142*, 15371−15385.
(30) Schaap-Oziemlak, A. M.; Kühn, P. T.; van Kooten, T. G.; van Rijn, P. Biomaterial-Stem Cell Interactions and Their Impact on Stem Cell Response. *RSC Adv.* **2014**, *4*, 53307−53320.
(31) Hollister, S. J. Porous Scaffold Design for Tissue Engineering. *Nat. Mater.* **2005**, *4*, 518−524.
(32) Chaudhuri, O.; Gu, L.; Klumpers, D.; Darnell, M.; Bencherif, S. A.; Weaver, J. C.; Huebsch, N.; Lee, H.; Lippens, E.; Duda, G. H.; Mooney, D. J. Hydrogels with Tunable Stress Relaxation Regulate Stem Cell Fate and Activity. *Nat. Mater.* **2016**, *15*, 326−334.
(33) Koski, K. J.; Akhenblit, P.; McKiernan, K.; Yarger, J. L. Non-Invasive Determination of the Complete Elastic Moduli of Spider Silks. *Nat. Mater.* **2013**, *12*, 262−267.
(34) Wu, Y.; Shah, D. U.; Wang, B.; Liu, J.; Ren, X.; Ramage, M. H.; Scherman, O. A. Biomimetic Supramolecular Fibers Exhibit Water-Induced Supercontraction. *Adv. Mater.* **2018**, *30*, 1707169.

https://dx.doi.org/10.1021/jacs.0c09691
J. Am. Chem. Soc. XXXX, XXX, XXX−XXX